Camphene. 5. Torsion Factors Influencing Exo/Endo Nametkin Rearrangement. The Structure of (−)-Camphene-8-carboxylic Acid[1]

Paul C. Moews, James R. Knox, and Wyman R. Vaughan*

Contribution from the Departments of Biological Sciences and Chemistry and the Institute of Materials Science, University of Connecticut, Storrs, Connecticut 06268. *Received July 20, 1977*

Abstract: The crystal and molecular structure of (−)-camphene-8-carboxylic acid, $C_{11}H_{16}O_2$, has been determined by direct phasing methods from x-ray diffraction data and refined by least squares to a residual of 4.8% for 1383 observed reflections. The compound crystallizes in the triclinic space group $P1$ with $a = 7.429$, $b = 12.020$, $c = 6.081$ Å, $\alpha = 98.06$, $\beta = 104.86$, $\gamma = 88.63°$, and $Z = 2$. Both molecules in the cell are similarly distorted in a manner consistent with preferential exo-methyl group migration in a Nametkin-type scheme of racemization of camphene. Dihedral angles involving the two methyl groups at C(3) are unequal, and differ from the ideal 60° value by more than eight times their calculated error; the angle C(8)C(2)-C(3)C(9) is 65.1° while C(8)C(2)-C(3)C(10) is 55.7°. This *gem*-dimethyl conformation could conceivably facilitate better overlap of an exo methyl σ orbital with the p orbital on C(2) in the transition state during rearrangement to the enantiomer.

Introduction

Camphene (**1**) and related bicyclic terpenoid compounds have been studied with a variety of objectives and over a long period of time.[2] One of us has investigated at some length[3-6] the nature of the processes by which optically active camphene racemizes and has identified and estimated the extent of participation of four distinctive pathways. These include two Nametkin-type rearrangements in which acid catalysis induces migration of either of the two methyl groups attached to C(3).

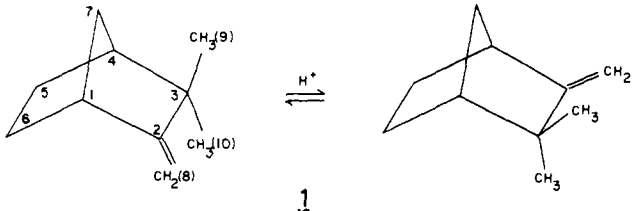

1

The remaining methyl group then loses a proton to produce the enantiomer of the original camphene. In the transition state the p orbital of C(2) is rehybridizing to a σ orbital while one of the σ orbitals (C(3)/C(9) or C(3)/C(10)) is rehybridizing to a p orbital on C(3). Schleyer[7] has used covalent systems, e.g., norbornene epoxide and tricyclo[3.2.1.$0^{2,4}$]octane, to argue that the presumed transition states (endo and exo) differ from each other by as much as 6 kcal/mol, and he has attributed this striking difference to skewing in the exo transition state (bond C(1)-C(2) and C(3)-C(4)) or eclipsing in the endo transition state (same bonds). His arguments are cogent but need not, indeed probably do not, exclude substantial enhancement of this presumed effect by nonbonded interactions.

What is particularly striking about these rearrangements is that the process involving C(9) migration is overwhelmingly the preferred mode of behavior, very little of the process involving C(10) being detectable in camphene itself.[5] This preference has broadly been attributed to steric factors,[7] but we feel that stereoelectronic better describes the situation, for an explanation of preferential exo migration (i.e., C(9)) must be sought not only in the molecular structure and inherent strains of the camphene system but also in the nature of the orbitals involved in the rearrangement. The volatility of camphene (**1**) has so far frustrated our efforts to crystallize it for x-ray structural study. The successful crystallization of the 8-carboxylic acid derivative **2** allowed us to study the conformation of a more stable camphene.[8] We now relate our crystallographic findings to earlier explanations of the rearrangement mechanism,[2-7] and we will attempt to show that these new results support the exo-migration pathway.

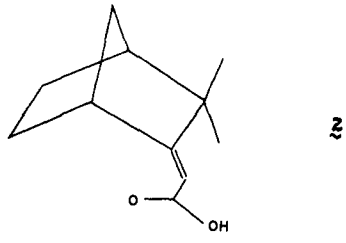

2

Experimental Section

Crystals of (−)-camphene-8-carboxylic acid (**2**) from petroleum ether were those described by Vaughan et al.[6] The crystallographic space group was determined to be $P1$ or $P\bar{1}$ from Weissenberg and precession photographs; as **2** is optically active the space group must be $P1$. The lattice parameters were refined by a least-squares fitting of diffractometer data for 12 centered reflections.

Crystal Data. $C_{11}H_{16}O_2$; mol wt 180.2; $F(000) = 196$; triclinic; $a = 7.429 \pm 0.002$, $b = 12.020 \pm 0.003$, $c = 6.081 \pm 0.002$ Å, $\alpha = 98.06 \pm 0.02$, $\beta = 104.86 \pm 0.03$, $\gamma = 88.63 \pm 0.02°$; volume = 519.6 Å^3; $d_c = 1.15$ g cm^{-3} for $Z = 2$; $d_m = 1.13$ g cm^{-3} by flotation. No systematic extinctions. Space group $P1$ (no. 1, C_1^1).

Since **2** slowly sublimes, the crystal used for data collection was sealed in a quartz capillary and cooled to 5 °C. Intensity data were collected with Cu Kα radiation ($\lambda = 1.542$ Å) on a Picker FACS-1 four-circle diffractometer with 1° min^{-1} 2θ scans (2° wide) and stationary 20-s background counts on either side of the scan. Three standard reflections were monitored every 150 reflections; no appreciable deterioration of the crystal was observed. Intensities for 1523 unique reflections were measured within the 2θ range 1-120°. Of these, 140 reflections had background-corrected intensities I_0 less than $4\sigma(I_0)$. These were assigned an intensity of $I_0 + 4\sigma(I_0)$ and were treated as unobserved. The standard deviation of the intensity $\sigma(I_0)$ was estimated to be $[CN + BG + (0.04I_0)^2]^{1/2}$ where CN is the peak count, BG is the total background count, and 0.04 is an estimated instrument stability factor. Corrections were made for Lorentz-polarization effects but not for absorption.

Structure Determination and Refinement. The structure was solved by direct methods using the program MULTAN.[9] Normalized structure factors were calculated from the 1383 observed data and the 298 E values greater than 1.4 used to calculate a number of E maps. The reflections used to define the origin were 1 3 3, 0 4 3, and 1 2 2; the enantiomorph was fixed by the 3 $\bar{9}$ 0 reflection.

Least-squares refinement of the structure was carried out with the program XRAY-72;[10] the quantity minimized was $\Sigma w(|F_o| - |F_c|)^2$

0002-7863/78/1500-0260$01.00/0

Table I. Fractional Coordinates ($\times 10^4$) and Anisotropic Temperature Factor Coefficients ($\times 10^3$)[a]

	x	y	z	U_{11}	U_{22}	U_{33}	U_{12}	U_{13}	U_{23}
				Molecule A					
C(1)	−995 (6)	2195 (4)	−1821 (8)	532 (25)	592 (26)	652 (27)	91 (20)	244 (21)	206 (21)
C(2)	618 (6)	1413 (3)	−1341 (7)	439 (21)	465 (22)	499 (22)	8 (17)	122 (17)	96 (17)
C(3)	2224 (6)	1930 (4)	−1991 (8)	544 (25)	481 (22)	615 (25)	−59 (19)	179 (20)	123 (19)
C(4)	1231 (7)	2978 (4)	−2996 (10)	729 (32)	552 (27)	884 (35)	−21 (23)	314 (28)	288 (25)
C(5)	−230 (9)	2609 (6)	−5239 (10)	918 (41)	944 (41)	649 (32)	195 (32)	127 (28)	325 (29)
C(6)	−1759 (8)	2031 (5)	−4449 (10)	647 (31)	937 (38)	717 (32)	72 (27)	71 (25)	309 (29)
C(7)	5 (8)	3330 (4)	−1364 (10)	798 (34)	486 (25)	853 (34)	136 (22)	263 (28)	188 (24)
C(8)	765 (8)	459 (4)	−454 (10)	432 (22)	476 (24)	728 (28)	27 (18)	146 (20)	195 (21)
C(9)	3804 (7)	2318 (5)	186 (11)	576 (29)	654 (31)	945 (36)	−175 (23)	72 (26)	82 (27)
C(10)	3041 (8)	1129 (5)	−3641 (10)	704 (32)	775 (34)	800 (35)	100 (25)	335 (27)	196 (27)
C(11)	−663 (6)	−61 (4)	339 (8)	483 (25)	517 (25)	703 (28)	0 (19)	119 (21)	197 (21)
O(1)	−152 (5)	−866 (3)	1513 (8)	555 (20)	737 (23)	1318 (32)	54 (17)	238 (20)	636 (23)
O(2)	−2320 (5)	266 (4)	−103 (8)	460 (20)	763 (24)	1159 (31)	24 (18)	215 (19)	469 (23)
				Molecule B					
C(1)	−3655 (7)	−3277 (5)	6044 (12)	641 (33)	776 (37)	1095 (43)	83 (27)	242 (31)	470 (33)
C(2)	−5426 (7)	−2709 (4)	4887 (9)	587 (27)	472 (24)	727 (29)	−53 (20)	139 (22)	110 (22)
C(3)	−7005 (7)	−3316 (4)	5463 (10)	573 (27)	604 (29)	789 (31)	−32 (22)	200 (24)	148 (24)
C(4)	−5881 (9)	−4211 (5)	6874 (12)	961 (42)	628 (32)	1050 (43)	−12 (28)	442 (36)	325 (31)
C(5)	−5193 (11)	−5077 (5)	5304 (15)	178 (55)	621 (35)	1436 (64)	61 (35)	614 (50)	234 (37)
C(6)	−3702 (11)	−4451 (6)	4603 (15)	268 (57)	907 (45)	1226 (51)	515 (40)	702 (45)	478 (40)
C(7)	−4115 (10)	−3567 (6)	8175 (12)	832 (39)	1063 (47)	862 (39)	178 (34)	91 (31)	437 (35)
C(8)	−5662 (6)	−1855 (4)	3704 (8)	506 (25)	526 (26)	676 (27)	21 (20)	122 (21)	i77 (22)
C(9)	−7948 (9)	−2528 (5)	6987 (12)	802 (37)	835 (39)	935 (39)	58 (29)	357 (31)	151 (31)
C(10)	−8482 (9)	−3761 (6)	3295 (12)	737 (36)	874 (41)	1040 (43)	−317 (32)	219 (32)	−11 (34)
C(11)	−4201 (7)	−1318 (4)	2999 (9)	568 (28)	452 (25)	815 (31)	7 (20)	101 (23)	251 (22)
O(1)	−4735 (5)	−536 (3)	1755 (7)	580 (21)	771 (25)	1147 (31)	65 (18)	184 (21)	527 (23)
O(2)	−2526 (5)	−1604 (4)	3528 (9)	499 (22)	885 (27)	1274 (35)	68 (20)	166 (22)	660 (27)

[a] The expression is $T = \exp[-2\pi^2(a^{*2}U_{11}h^2 + b^{*2}U_{22}k^2 + c^{*2}U_{33}l^2 + 2a^*b^*U_{12}hk + 2a^*c^*U_{13}hl + 2b^*c^*U_{23}kl)]$. Standard deviations are given in parentheses.

where $w = \sigma^{-2}(F_o)$. Unobserved reflections were omitted from the refinement. The positions of the 26 atoms other than hydrogen together with their isotropic temperature factors were parameters in the first cycles of refinement; on convergence the residual $\Sigma||F_o| - |F_c||/\Sigma|F_o|$ was 17.2%. Five cycles of anisotropic temperature factor refinement brought the residual to 8.4%, and a difference Fourier map was calculated to locate the 32 hydrogen atoms. The map contained 35 peaks which ranged in value from 0.17 to 0.39 e/Å; of these, 28 were in positions expected for the 32 hydrogen atoms. The hydroxyl hydrogen atom of each molecule and the two hydrogen atoms bonded to C(6) of molecule B could not be located at this stage. The 28 hydrogen atoms were included in the next cycle of refinement though their positions were not varied. A second difference Fourier map revealed the two hydrogen atoms bonded to oxygen as the two highest peaks, and it showed one of the atoms bonded to C(6) of molecule B as the fourth highest peak. The other hydrogen atom bonded to C(6) was assigned its expected position and refinement continued. On convergence of anisotropic refinement of the nonhydrogen atoms only, the residual dropped to 5.9%. One additional cycle of refinement was carried out in which hydrogen positions and isotropic temperature factors were varied, but shifts were restricted to 60% of their calculated values. The average C-H bond distance changed from 1.05 Å to 1.01 Å, while the average tetrahedral valence angle involving hydrogen remained constant at 111° during this last cycle of refinement. The final residual was 4.8%, and parameter shifts were less than 0.5σ. Final atomic coordinates are given in Tables I and II; observed and calculated structure factors have been deposited (see supplementary material).

Discussion of Results

Crystal Structure. The packing of the molecules is shown in Figure 1. The two molecules in the triclinic cell are crystallographically independent, yet closely related by a pseudocenter of symmetry located between the carboxyl groups. All atoms except C(5,6,7) obey the centrosymmetry to within 0.5 Å, and this positional relatedness led to considerable difficulty in solving the structure. Two strong hydrogen bonds (each 2.62 Å) involving the carboxyl groups form the molecules into dimers held in the crystal lattice solely by van der Waals

Table II. Fractional Coordinates ($\times 10^3$) of Hydrogen Atoms and Isotropic Temperature Factors ($\times 10^3$)[a]

Atom	x	y	z	U
		Molecule A		
H(C1)	−168 (6)	218 (4)	−96 (7)	46 (11)
H(C4)	223 (6)	357 (4)	−310 (8)	75 (11)
H1(C5)	8 (6)	204 (4)	−659 (8)	67 (11)
H2(C5)	−97 (6)	327 (4)	−588 (7)	71 (11)
H1(C6)	−191 (6)	119 (4)	−500 (7)	62 (11)
H2(C6)	−293 (6)	236 (4)	−494 (7)	73 (11)
H1(C7)	57 (6)	357 (4)	35 (7)	61 (11)
H2(C7)	−59 (6)	393 (4)	−177 (7)	67 (11)
H(C8)	191 (7)	3 (4)	−26 (8)	66 (11)
H1(C9)	327 (7)	287 (4)	146 (8)	67 (12)
H2(C9)	470 (7)	278 (4)	−3 (8)	75 (12)
H3(C9)	432 (7)	166 (4)	100 (8)	76 (12)
H1(C10)	358 (7)	49 (4)	−303 (8)	65 (12)
H2(C10)	361 (7)	141 (4)	−462 (8)	80 (11)
H3(C10)	197 (7)	75 (4)	−497 (8)	68 (11)
H(01)	−100 (7)	−107 (4)	246 (8)	96 (11)
		Molecule B		
H(C1)	−236 (6)	−282 (4)	599 (7)	79 (11)
H(C4)	−654 (6)	−459 (4)	780 (7)	61 (11)
H1(C5)	−471 (6)	−583 (4)	616 (7)	81 (11)
H2(C5)	−625 (6)	−537 (4)	390 (8)	82 (11)
H1(C6)	−264 (6)	−483 (4)	496 (7)	74 (11)
H2(C6)	−394 (6)	−437 (4)	292 (7)	72 (11)
H1(C7)	−434 (6)	−288 (4)	948 (8)	70 (11)
H2(C7)	−349 (6)	−400 (4)	874 (8)	65 (11)
H(C8)	−694 (7)	−148 (4)	333 (8)	66 (12)
H1(C9)	−853 (7)	−184 (4)	614 (8)	72 (12)
H2(C9)	−889 (7)	−300 (4)	739 (8)	78 (11)
H3(C9)	−695 (7)	−209 (4)	840 (8)	72 (12)
H1(C10)	−800 (7)	−417 (4)	185 (8)	72 (12)
H2(C10)	−951 (7)	−410 (4)	378 (8)	67 (12)
H3(C10)	−923 (6)	−308 (4)	234 (8)	65 (12)
H(01)	−354 (6)	−16 (4)	95 (7)	113 (12)

[a] The expression used is $T = \exp(-8\pi^2 U \sin^2\theta/\lambda^2)$.

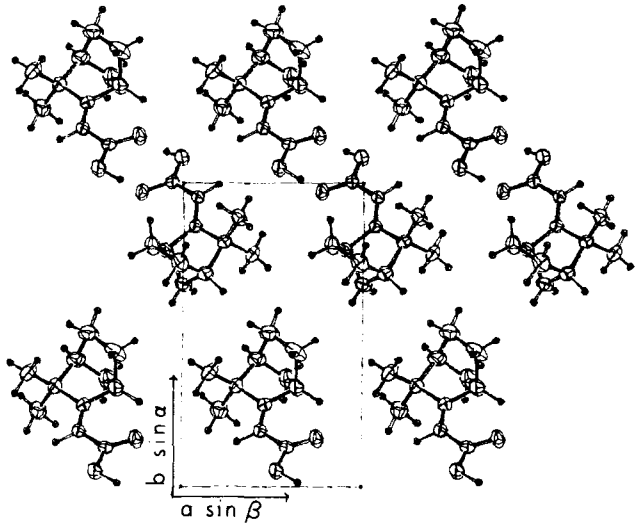

Figure 1. Projection of structure along the *c* axis.

forces. Consequently the crystals slowly sublime at room temperature, though not as rapidly as the noncarboxylated parent camphene.

Orientational disorder occurs in the carboxyl groups. These groups adopt primarily the syn-planar conformation a, with the occasional occurrence of conformation b throughout the crystal. Were the disorder complete, with equal occurrence of a and b, the two C–O bond lengths (Table III) would be equal. Incomplete packing disorder in this carboxylic acid correlates with the findings of Leiserowitz.[11] He saw that while α,β-

a b

saturated carboxylic acids always adopt the syn-planar arrangement, α,β-*un*saturated carboxylic acids such as **2** occur in *both* the syn-planar a and anti-planar b forms. This disorder is believed to be static[11] in that no proton transfer occurs across the OH-O bond. In a statically disordered crystal in which a and b occur, oxygen atom positions would be separated by about 0.1 Å, leading to high crystallographic temperature factors. The calculated temperature factors of the oxygen atoms in **2** are in fact higher than those of the other atoms, supporting the view of static disorder. Thermal ellipsoids are seen in Figures 1 and 2.

Molecular Conformation. The two independent molecules in the unit cell are quite similar in conformation, and can be superposed to within 0.05 Å in atomic positions. Figure 2 is a stereoview of the molecules. Corresponding bond distances and angles (Table III) in the two molecules are equivalent, each differing no more than 3σ from the average. Two torsion angles about the C(2)-C(3) bond show significant deviations from 60° values expected from Dreiding models. It can be seen from Table IV that the methyl torsion angles C(8)C(2)-C(3)C(9) and C(8)C(2)-C(3)C(10) deviate from 60° by 4-7°, more than eight or ten times their calculated error of 0.5°. For each of these torsion angles, the direction of the twist is the same in *both* of the crystallographically independent molecules, confirming the reality of the distortion. This finding will be discussed later in terms of a Nametkin rearrangement scheme for methyl migration.

Because the molecule's carboxyl group is ideally coplanar with the sp^2 orbitals of the double-bonded C(2) atom, an asymmetric angular distortion appears at C(2) such that angle C(1)C(2)C(8) is 5-7° larger than C(3)C(2)C(8) in both molecules (Figure 3). This is a result of contact between the

Table III. Bond Distances (Å) and Angles (deg) in (−)-Camphene-8-carboxylic Acid[a]

	Molecule A	Molecule B
	Bond Lengths	
C(1)-C(6)	1.538 (7)	1.549 (9)
C(1)-C(2)	1.499 (12)	1.519 (14)
C(2)-C(3)	1.520 (7)	1.534 (8)
C(3)-C(4)	1.564 (7)	1.561 (8)
C(4)-C(5)	1.526 (7)	1.485 (11)
C(5)-C(6)	1.554 (10)	1.532 (13)
C(4)-C(7)	1.523 (9)	1.513 (9)
C(1)-C(7)	1.525 (7)	1.509 (11)
C(3)-C(9)	1.551 (7)	1.518 (9)
C(3)-C(10)	1.521 (8)	1.522 (8)
C(2)-C(8)	1.325 (8)	1.318 (14)
C(8)-C(11)	1.459 (10)	1.458 (8)
C(11)-O(1)	1.275 (6)	1.281 (6)
C(11)-O(2)	1.257 (6)	1.256 (6)
	Valence Angles	
C(6)-C(1)-C(7)	102.3 (5)	101.6 (6)
C(2)-C(1)-C(6)	105.7 (4)	105.1 (5)
C(2)-C(1)-C(7)	101.3 (4)	102.0 (5)
C(1)-C(2)-C(3)	107.2 (4)	105.0 (4)
C(1)-C(2)-C(8)	130.0 (4)	130.4 (5)
C(3)-C(2)-C(8)	122.8 (3)	124.6 (4)
C(2)-C(3)-C(9)	110.4 (4)	110.9 (4)
C(2)-C(3)-C(10)	113.4 (4)	111.2 (5)
C(4)-C(3)-C(9)	109.7 (4)	109.5 (5)
C(4)-C(3)-C(10)	115.2 (4)	116.7 (4)
C(2)-C(3)-C(4)	99.8 (4)	100.7 (4)
C(9)-C(3)-C(10)	108.4 (4)	107.8 (4)
C(3)-C(4)-C(5)	110.4 (4)	109.3 (6)
C(3)-C(4)-C(7)	101.4 (5)	102.0 (5)
C(5)-C(4)-C(7)	101.3 (5)	102.3 (6)
C(4)-C(5)-C(6)	103.4 (5)	103.6 (5)
C(5)-C(6)-C(1)	102.3 (4)	102.5 (7)
C(1)-C(7)-C(4)	94.3 (4)	94.5 (5)
C(2)-C(8)-C(11)	126.4 (3)	125.4 (4)
C(8)-C(11)-O(1)	116.9 (3)	115.7 (4)
C(8)-C(11)-O(2)	121.8 (4)	123.1 (4)
O(1)-C(11)-O(2)	121.3 (5)	121.2 (5)

[a] Standard deviations are given in parentheses.

hydrogen atom of C(1) and the oxygen atom O(2) in the carboxyl group, the carbonyl bond of which is predominantly cis to the carbon-carbon double bond, as seen by Leiserowitz[11] in many α,β-unsaturated carboxylic acids. The hydrogen contact to O(2) is closest in the B molecule (2.21 Å); in the A molecule the contact is longer (2.51 Å) because the carboxyl group has rotated away from the hydrogen atom. Thus, in molecule A the torsion angle C(2)C(8)-C(11)O(2) is 12° from the syn-planar conformation while in molecule B the torsion angle about C(8)-C(11) is very nearly syn-planar (−1°). The B molecule instead twists 7.5° about the unsaturated carbon-carbon bond as a result of its close H···O contact.

Covalent bond angles about atoms C(3) and C(4) show a pattern which can be attributed to the methyl substituents at C(3). In (a) of the schematic shown below, the dashed lines show approximate torsion angles about C(3)-C(4) estimated from a Drieding model which does not take into account the van der Waals size of the atoms. Our results show that to relieve unfavorable contact between C(5) and C(10), the

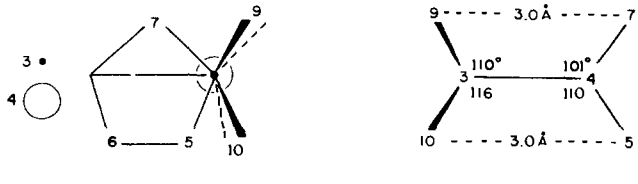

a b

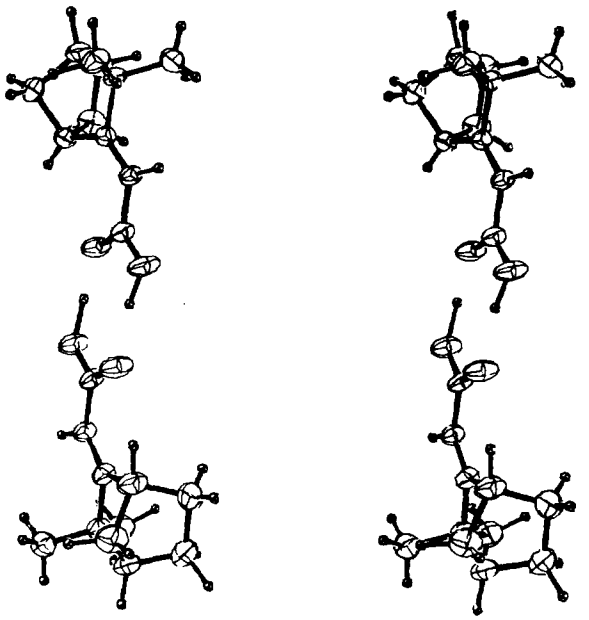

Figure 2. Stereoscopic view of **2** showing elongation of oxygen atom thermal ellipsoids.

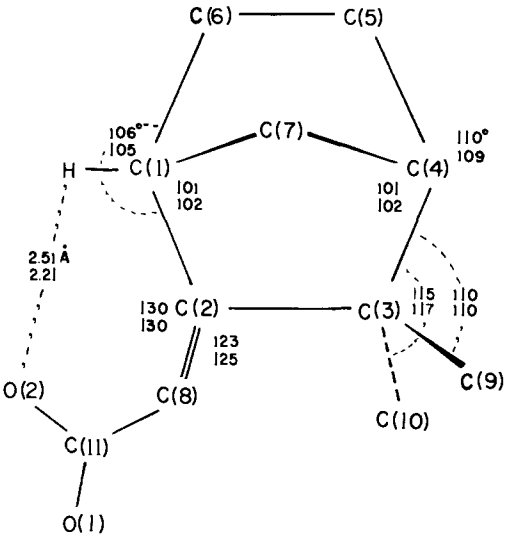

Figure 3. Schematic showing selected bond angles and O(2) · · ·HC(1) distances in molecule A (above) and B (below).

methyl-group bonds have rotated about 5° until their contacts to C(5) and C(7) are *equal* at 3.0 Å. While the resultant C(9)C(3)-C(4)C(7) twist places the C(9) methyl group 79° from C(7), the C(10)C(3)-C(4)C(5) twist places the C(10) methyl only 51° away from C(5). Consequently, the two covalent bond angles involving C(10) and C(5) must expand relative to those involving C(9) and C(7), as seen in schematic (b). The C(10)C(3)C(4) angle is distorted more than the C(3)C(4)C(5) angle because the terminal C(10) methyl group is less constrained than the C(5) carbon in the rigid cage structure. This C(3)C(4)C(5) angle is still, however, 4° (or 8σ) larger than the chemically equivalent C(2)C(1)C(6) angle on the unsubstituted side of the cage (Figure 3).

On the Nametkin Rearrangement. Insight into the geometrical situation may be gained from consideration of a projection down the C(2)-C(3) bond which may be used to picture the *gem*-dimethyl system. It will be noted that the ideal dihedral or torsion angles α and β are ~60° (C(8)C(2)-C(3)C(9) and C(8)C(2)-C(3)C(10)), and this should result in approximately

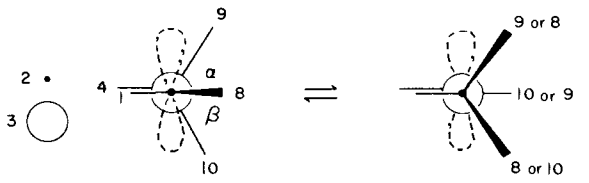

equal barriers to migration of C(9) and C(10). If the *gem*-dimethyl system could be "twisted" about the C(2)-C(3) bond in either direction, either C(9) or C(10) migration would be favored, depending on which σ bond becomes more nearly parallel with the p orbital on C(2). At the same time the nonmigrating methyl group would be closer to its ultimate position. A decrease in α and a concurrent increase in β would facilitate endo (C(10)) migration. Such distortion could be induced by increasing the size of C(9) (e.g., by making it an ethyl group) so that there is stronger repulsion against syn-H on C(7). This has been observed;[6] and the reverse substitution (ethyl instead of methyl at C(10)) should increase the relative rate of C(9) methyl migration compared to that in camphene itself. This too has been observed.[6]

Thus we are in a position to suggest that the inherent preference for C(9) methyl (exo) migration may be attributed (at least in part) to unequal dihedral angles (α and β) in the camphene system induced by unequal nonbonded interactions between C(9) and syn H-7 as compared to C(10) and endo H-5 in a framework model which does not take into account the van der Waals radii of the atoms involved. Such radii suggest a minimum approach distance of two hydrogen atoms to be 2.2 Å and of a methyl group and a hydrogen atom to be 3.0 Å. But in a Dreiding model of the axial conformer of methylcyclohexane (chair form) the corresponding shortest distances of approach are respectively ~1.8 and 2.6 Å. And in such a conformer the nonbonded interactions of the axial methyl group with the 3- and 5-cis-hydrogen atoms are sufficiently strong to prevent the existence of any substantial numbers of the axial chair conformer in equilibrium with the equatorial chair conformer. Since the axial conformer of methylcyclohexane

Table IV. Torsion Angles (deg) in (−)-Camphene-8-carboxylic Acid[a]

Atoms	Molecule A	Molecule B
C(6)C(1)-C(2)C(3)	74.8	72.0
C(6)C(1)-C(2)C(8)	−107.2	−110.5
C(7)C(1)-C(2)C(3)	−31.6	−33.7
C(7)C(1)-C(2)C(8)	146.4	143.9
C(8)C(2)-C(3)C(9)	−66.7	−63.5
C(8)C(2)-C(3)C(10)	55.0	56.4
C(1)C(2)-C(3)C(9)	111.4	114.3
C(1)C(2)-C(3)C(10)	−126.9	−125.9
C(1)C(2)-C(3)C(4)	−4.0	−1.6
C(8)C(2)-C(3)C(4)	177.9	−179.3
C(9)C(3)-C(4)C(5)	175.7	171.7
C(10)C(3)-C(4)C(5)	53.2	49.0
C(9)C(3)-C(4)C(7)	−77.6	−80.6
C(10)C(3)-C(4)C(7)	159.8	156.7
C(2)C(3)-C(4)C(5)	−68.3	−71.5
C(2)C(3)-C(4)C(7)	38.4	36.3
C(3)C(4)-C(5)C(6)	69.4	69.8
C(7)C(4)-C(5)C(6)	−37.3	−37.8
C(4)C(5)-C(6)C(1)	2.4	3.4
C(5)C(6)-C(1)C(2)	−72.3	−73.9
C(5)C(6)-C(1)C(7)	33.3	32.1
C(1)C(2)-C(8)C(11)	−1.5	7.5
C(3)C(2)-C(8)C(11)	176.2	−175.3
C(2)C(8)-C(11)O(1)	−167.6	176.5
C(2)C(8)-C(11)O(2)	−12.2	−1.1

[a] Zero angle is defined with front and rear bond superposed in projection down middle bond. Angle is positive if right-hand rotation of either bond is required for their superposition.

may, however, exist at equilibrium to the extent of 5%,[12] it is reasonable to suppose that the same nearness of approach of a methyl group (or its hydrogen atoms) and a hydrogen atom (measured in the Dreiding model of axial methylcyclohexane) can be tolerated in the camphene system between C(9) and syn-H-7 provided that there is enough strain elsewhere to hold the nonbonded atoms in place.

Where the nearness of approach is *less* than in axial methylcyclohexane there is going to be considerable repulsion. The resultant strain can best be relieved by a twisting of the *gem*-dimethyl system about the C(2)-C(3) bond in a direction which increases the C(10)/endo-H-5 distance while decreasing the C(9)/exo-H-7 distance until a satisfactory balance of nonbonded interactions and resultant strains is achieved. Such twisting should result in an increase in the torsion angle for C(9) (α) and a corresponding decrease in the corresponding angle for C(10) (β). And as a consequence the σ orbital for C(3)-C(9) becomes more nearly parallel to the p orbital for C(2), thus allowing better orbital overlap in approaching the transition state for rearrangement while at the same time bringing the C(3)-C(10) σ orbital less nearly parallel to the p orbital of C(2), thus disfavoring effective orbital overlap in approaching the transition state for C(10)/C(2) migration. Furthermore, as noted above, this twisting positions C(10) closer to its final position, which should favor the overall rearrangement process.

Until now the only support for the effects of unequal nonbonded interactions in favoring exo at the expense of endo alkyl migration has been the rate studies involving three homocamphenes in which exo-methyl migration is enhanced by an endo ethyl group, and exo-ethyl migration is slower than exo-methyl migration.[6] But with the present x-ray diffraction data which clearly demonstrate an increase in the torsion angle α and a concomitant decrease in the torsion angle β, there is strong support for the postulated twisting. Thus it is possible to offer this crystallographic finding as entirely consistent with the kinetic data on the three homocamphenes and as the source of the strong preference for exo-methyl migration over endo-methyl migration[5] in the racemization of camphene via the Nametkin rearrangement.

Supplementary Material Available: List of structure factors for (−)-camphene-8-carboxylic acid (16 pages). Ordering information is given on any current masthead page.

References and Notes

(1) Publication 923 from the Institute of Materials Science, University of Connecticut. Financial support was provided by the National Institute of Allergies and Infectious Diseases (Grant AI-10925). Computations were performed at the University of Connecticut Computer Center.
(2) For a brief discussion and leading references see J. Simonsen, "The Terpenes", Vol. II, 2nd ed, Cambridge University Press, New York, N.Y., 1949, pp 290–293.
(3) W. R. Vaughan and R. Perry, Jr., *J. Am. Chem. Soc.*, **75**, 3168–3172 (1953).
(4) W. R. Vaughan, C. T. Goetschel, M. H. Goodrow, and C. L. Warren, *J. Am. Chem. Soc.*, **85**, 2282–2289 (1963).
(5) C. W. David, B. W. Everling, R. J. Killan, J. B. Stochers, and W. R. Vaughan, *J. Am. Chem. Soc.*, **95**, 1265–1270 (1973).
(6) W. R. Vaughan and D. M. Teegarden, *J. Am. Chem Soc.*, **96**, 4902–4909 (1974).
(7) P. v. R. Schleyer, *J. Am. Chem. Soc.*, **89**, 699–701 (1967).
(8) P. C. Moews, J. R., Knox, and W. R. Vaughan, *Tetrahedron Lett.*, 359–362 (1977).
(9) G. Germain, P. Main, and M. M. Woolfson, *Acta Crystallogr., Sect. A*, **27**, 368–376 (1971).
(10) J. M. Stewart, G. J. Kruger, H. L. Ammon, C. Dickinson, and S. R. Hall, Technical Report TR-192, Computer Science Center, University of Maryland, 1972.
(11) L. Leiserowitz, *Acta Crystallogr., Sect. B*, **32**, 775–802 (1976).
(12) F. R. Jensen and L. H. Gale, *J. Org. Chem.*, **25**, 2075–2078 (1960).

Transition Metal Catalyzed Asymmetric Organic Syntheses via Polymer-Attached Optically Active Phosphine Ligands. Synthesis of *R* Amino Acids and Hydratropic Acid by Hydrogenation[1]

Naotake Takaishi, Hirosuke Imai, Christopher A. Bertelo, and J. K. Stille*[2]

Contribution from the Department of Chemistry, University of Iowa, Iowa City, Iowa 52242.

Received June 13, 1977

Abstract: The reaction of (−)-1,4-ditosylthreitol (**2**) with 4-vinylbenzaldehyde afforded 2-*p*-styryl-4,5-bis(tosyloxymethyl)-1,3-dioxolane (**3**), which was copolymerized (radical) with hydroxyethyl methacrylate to incorporate 8 mol % **3** in the cross-linked copolymer **4.** Treatment of **4** with enough sodium diphenylphosphide to react with all the hydroxyl functions plus the tosylate groups gave a hydrophilic polymer (**5**) (after neutralization) bearing the optically active 4,5-bis(diphenylphosphinomethyl)-1,3-dioxolane ligand. Exchange of rhodium(I) onto **5** with $[(C_2H_4)_2RhCl]_2$ gave the polymer-attached catalyst **6,** that would swell in alcohol and other polar solvents. Hydrogenation of α-*N*-acylaminoacrylic acids in ethanol with this catalyst gave the amino acid derivatives having the same optical yields and absolute configuration as could be obtained with the homogeneous analogue. The catalyst could be removed by filtration and reused with no loss of optical purity in the hydrogenated product.

Introduction

Of the methods of synthesis of optically active organic compounds, the generation of an optically active product from a prochiral reactant by use of an optically active catalyst or enzyme has several advantages, the most important of which is that either an available, naturally occurring catalyst or enzyme is utilized, or resolution is achieved with the catalyst instead of with the product. When resolution is carried out with the catalyst, only small quantities of resolved material are necessary; product resolution often results in loss of one enantiomer and possibly the resolving agent.[3]

Homogeneously catalyzed reactions generally take place at lower temperatures and pressures and are more selective. Because of this, homogeneously catalyzed reactions have

0002-7863/78/1500-0264$01.00/0